Published in final edited form as:
Transl Stroke Res. 2011 March 1; 2(1): 72–79. doi:10.1007/s12975-010-0052-2.

Subarachnoid Hemorrhage Induces Gliosis and Increased Expression of the Pro-inflammatory Cytokine High Mobility Group Box 1 Protein

Kentaro Murakami,
Department of Pharmacology, University of Vermont College of Medicine, 89 Beaumont Ave., Burlington, VT 05405, USA

Masayo Koide,
Department of Pharmacology, University of Vermont College of Medicine, 89 Beaumont Ave., Burlington, VT 05405, USA

Travis M. Dumont,
Department of Surgery, Division of Neurosurgery, University of Vermont College of Medicine, Burlington, VT, USA

Sheila R. Russell,
Department of Surgery, Division of Neurosurgery, University of Vermont College of Medicine, Burlington, VT, USA

Bruce I. Tranmer, and
Department of Surgery, Division of Neurosurgery, University of Vermont College of Medicine, Burlington, VT, USA

George C. Wellman
Department of Pharmacology, University of Vermont College of Medicine, 89 Beaumont Ave., Burlington, VT 05405, USA; Department of Surgery, Division of Neurosurgery, University of Vermont College of Medicine, Burlington, VT, USA

George C. Wellman: George.Wellman@uvm.edu

Abstract

Subarachnoid hemorrhage (SAH) following cerebral aneurysm rupture is associated with high rates of morbidity and mortality. Surviving SAH patients often suffer from neurological impairment, yet little is currently known regarding the influence of subarachnoid blood on brain parenchyma. The objective of the present study was to examine the impact of subarachnoid blood on glial cells using a rabbit SAH model. The astrocyte-specific proteins, glial fibrillary acidic protein (GFAP) and S100B, were up-regulated in brainstem from SAH model rabbits, consistent with the development of reactive astrogliosis. In addition to reactive astrogliosis, cytosolic expression of the pro-inflammatory cytokine, high-mobility group box 1 protein (HMGB1) was increased in brain from SAH animals. We found that greater than 90% of cells expressing cytosolic HMGB1 immunostained positively for Iba1, a specific marker for microglia and macrophages. Further, the number of Iba1-positive cells was similar in brain from control and SAH animals, suggesting the majority of these cells were likely resident microglial cells rather than infiltrating macrophages. These observations demonstrate SAH impacts brain parenchyma by

Correspondence to: George C. Wellman, George.Wellman@uvm.edu.

Disclosure The authors declare no conflicts of interest.

activating astrocytes and microglia, triggering up-regulation of the pro-inflammatory cytokine HMGB1.

Keywords

Subarachnoid hemorrhage; Reactive astrogliosis; Inflammation; Microglia; Vasospasm

Introduction

Cerebral aneurysm rupture and the ensuing release of blood into the subarachnoid space are associated with substantial morbidity and mortality. Overall mortality associated with aneurysmal SAH reaches 40–50% within the first 30 days, and the majority of survivors are left with moderate to severe neurological disabilities [1]. Despite the severity of this disorder, current treatments for SAH are relatively ineffective. For decades, vasospasm prevention of conduit cerebral arteries located within the blood clot on the brain surface has been the focus of therapeutic strategies utilized for SAH patients. However, the degree of angiographic vasospasm is not always well correlated with the development of neurological deficits in SAH patients, and other influences such as early brain injury due to cortical spreading depression, disruption of the blood–brain barrier, impaired function of the microcirculation, inflammation, and apoptotic cell death may contribute to SAH-induced pathologies [2–6].

Currently, the impact of SAH on brain parenchyma is not clear, particularly with respect to glial cells including astrocytes and microglia. Reactive astrogliosis characterized by up-regulation of the astrocyte-specific proteins GFAP and S100B is a common feature of many central nervous system pathologies including head trauma, ischemic stroke, neurodegenerative diseases, and cancer [7,8]. In SAH patients, GFAP and S100B are elevated in both CSF and serum [9–11] with high S100B levels in CSF correlated to poor 1-year clinical outcome [12]. Despite such clinically relevant information, surprisingly little is known regarding the development of reactive astrogliosis following SAH. Although the presence of reactive astrocytes following SAH was alluded to by Yokota et al. [13], detailed information regarding the development of SAH-induced reactive astrogliosis is lacking. Thus, it is unclear whether increased GFAP and S100B levels in the CSF and serum of SAH patients represent an up-regulation of protein due to the induction of reactive astrogliosis or an increase in their release into the extracellular space, reflecting astrocyte damage or cell death.

Another unresolved issue is the occurrence of brain parenchyma inflammation following SAH. Inflammation can represent an adaptive response following injury to promote tissue repair. However, both acute and chronic inflammation can also lead to further tissue damage and have been implicated in pathologies of the central nervous system, including SAH. Inflammation induced by extravascular blood within the subarachnoid space has been proposed to contribute to SAH-induced vasospasm of arteries on the brain surface [14]. Although relatively few studies have investigated SAH-induced inflammation within the brain [15,16], Prunell et al. [15] have shown that SAH can induce parenchymal expression of several cytokines including TNF-α. It has recently been reported that elevated CSF levels of the pro-inflammatory cytokine high-mobility group box 1 protein (HMGB1) are correlated with poor outcome in SAH patients [17,18]. HMGB1 is a non-histone DNA binding protein present in the nucleus of neurons, astrocytes, microglia, and oligodendrocyte-like cells under physiological conditions. However, during pathological events HMGB1 can be up-regulated, retained in the cytosol, and secreted by activated microglia as a pro-inflammatory cytokine [19,20]. Thus, increased levels of HMGB1 in the

CSF of SAH patients could reflect either secretion from activated microglia or passive diffusion from the nuclei of necrotic cells within the brain.

In the present study, we hypothesized that SAH impacts brain parenchyma, specifically glial cells, triggering astrogliosis and enhanced production of HMGB1. Our findings demonstrate that brain tissue from SAH animals exhibit increased GFAP and S100B expression, characteristic of reactive astrogliosis. In addition, our work suggests that cytosolic levels of pro-inflammatory HMGB1 are up-regulated in activated microglia after SAH. Together, these findings reveal that subarachnoid blood has a profound influence on glial cells within the brain that may contribute to the manifestation of neurological deficits following cerebral aneurysm rupture.

Materials and Methods

All studies were conducted in accordance with the *Guidelines for the Care and Use of Laboratory Animals* (NIH) and approved by the Institutional Animal Care and Use Committee of the University of Vermont.

SAH Model

New Zealand White rabbits (male, 3.0 to 3.5 kg), under isoflurane anesthesia, received an intracisternal injection of 3 ml of autologous arterial blood via the cisterna magna, as previously described [21,22]. Buprenorphine (0.01 mg/kg) was given every 12 h (for 36 h, then as needed) as an analgesic. At 48 h post-surgery, animals were either euthanized (2-day SAH study group) or received a second intracisternal injection of 3 ml of autologous arterial blood using the approach described above. These animals were euthanized 72 h after the second surgical procedure (5-day SAH study group). Sham-operated rabbits had the same surgical procedures as SAH animals with the exception that physiological saline (3 ml) was injected into the cisterna magna rather than autologous arterial blood. Throughout the course of this study, no animals died as a result of the surgical procedures. No scored evaluation of neurological deficits was performed on these animals. However, the animals were in general good health (e.g., ambulatory and eating) and did not exhibit overt signs of neurological deficits (e.g., head tilt, seizures) during routine postoperative checks. A group of un-operated animals were also used as controls. Animals were euthanized by exsanguination and decapitation under deep pentobarbital anesthesia (IV; 60 mg/kg body weight). Brains were placed in ice-cold, oxygenated physiological saline solution for further dissection. Brainstem tissue from the medulla oblongata located 1–2 mm below the ventral brain surface was used in this study (Fig. 1).

Immunohistochemistry

Brainstem tissue was fixed with 4% paraformaldehyde overnight and embedded in paraffin. Sections 10 μm in thickness were dewaxed and blocked with 5% normal donkey serum for 3 h at room temperature prior to incubation with anti-GFAP antibody (Sigma-Aldrich Co., St. Louis, MO, USA; mouse monoclonal IgG; 1:200) overnight at 4°C. Sections were then immunolabeled with secondary antibody (Invitrogen Corp., Carlsbad, CA, USA; Alexa Fluor 488 donkey anti-mouse IgG; 1:800) for 1 h at room temperature. HMGB1/Iba1 double immunostaining was performed using an antigen retrieval procedure. Briefly, dewaxed sections were boiled for 30 min in 0.01 M citrate buffer (pH 6.0) before blocking with 5% donkey serum (3 h) and incubation with primary antibodies (HMGB1 antibody, Sigma, mouse monoclonal IgG 1:100; Iba1 antibody, Abcam Inc., Cambridge, MA, USA; goat polyclonal IgG 1:200) overnight at 4°C, followed by immunolabeling with secondary antibodies (Alexa Fluor 488 donkey anti-mouse IgG; 1:800; Alexa Fluor 555 donkey anti-goat IgG; 1:800). Slow Fade with DAPI (Invitrogen) was applied to the sections and images

were captured using a DeltaVision restoration microscopy system attached to an Olympus IX70 microscope. Ten-micrometer optical sections in the *z*-axis were acquired in 0.5-μm steps using a 20× objective and identical settings were used for all sections. Images were deconvoluted using SoftWoRx software (Applied Precision Inc., Issaquah, WA, USA) and analyzed with ImageJ software (NIH).

Western Blotting

Brainstem tissue was homogenized in cold buffered solution containing 20 mM Tris–HCl (pH 7.4), 1 mM ethyl-enediaminetetraacetic acid (EDTA), 1 mM glycol-bis(2-aminoethylether)-*N*,*N*,*N*′,*N*′-tetraacetic acid (EGTA), 150 mM NaCl, 5 mM dithiothreitol containing 10 μM leupeptin, and 1 mM phenylmethanesulfonyl fluoride. Homogenates were solubilized in the presence of 1% sodium dodecyl sulfate for 30 min at 4°C then boiled for 10 min and stored at −20°C until used. Five micrograms of protein per sample, determined by Bradford assay with Coomassie Protein Assay kit (Pierce Biotechnology Inc., Rockford, IL, USA), were used for Western blot analysis. Briefly, the blotted membrane was blocked by Aquablock (EastCoast Bio Inc., North Berwick, ME, USA), washed with Tris-buffered saline containing 0.1% Tween-20 (TTBS), and incubated with the following primary antibodies: anti-GFAP mouse monoclonal antibody (1:500 in TTBS, clone G-A-5; Sigma) for 1 h at room temperature, anti-HMGB1 mouse monoclonal antibody (1:1,000 in TTBS, clone HAP46.5; Sigma) for 1 h at room temperature, and anti β-tubulin rabbit monoclonal antibody (1:1,000 in TTBS containing 3% bovine serum albumin, clone 9F3; Cell Signaling, Boston, MA, USA) overnight at 4°C. After washing with TTBS, the membrane was incubated with the appropriate secondary antibody for 2 h at room temperature; Alexa Flour 700 conjugated goat anti-mouse IgG antibody (1;10,000 in TTBS, Invitrogen) or peroxidase conjugated sheep anti-rabbit IgG antibody (1:10,000 in TTBS containing 5% nonfat dried milk; GE Healthcare, Piscataway, NJ, USA). The signals were detected by an Odyssey® infrared imaging system (LI-COR® Biosciences, Lincoln, NE, USA) for GFAP and HMGB1, or by chemiluminescence (SuperSignal®; Thermo Scientific, Rockford, IL, USA) for β-tubulin. Band intensity was quantified using NIH software (ImageJ) and expressed as a ratio to β-tubulin band intensity.

RNA Isolation and RT–PCR—Total RNA was extracted from brainstem tissue using RNeasy Micro kit (QIAGEN). cDNA was then synthesized by Omniscript reverse transcriptase (QIAGEN) using oligo-dT primers. The following primer sets (forward: reverse primer) were used: S100B—TCCATCAGTATTCGG-GAAGG: ATAGCGACGAAGGCC ATAAA (GenBank accession # AY0505681.1); HMGB-1—GTTCTGAG-TATCGCCCCAAA: TCCTCCTCATCCT CTTCGTC (Ensembl Transcript ID=ENSO CUT00000009280); and GAPDH—TGGCAAAGTGGATGTTGTCG: CATGGTGGTGAAGACGCCAG (GenBank accession # L23961.1). The PCR band intensity of the gene of interest was normalized to the house-keeping geneglyceraldehyde-3-phosphate dehydrogenase (GAPDH).

Statistical Analysis: Data are presented as mean±SEM. Statistical significance was considered at the level of $p < 0.05$ using Student's *t* test or one-way ANOVA followed by Tukey–Kramer multiple comparison test.

Results

Enhanced Expression of Glial Fibrillary Acidic Protein Following SAH

A prominent feature of reactive astrogliosis is increased expression of the astrocyte-specific intermediate filament, glial fibrillary acidic protein (GFAP) [23]. To investigate evidence of SAH-induced reactive astrogliosis, GFAP levels were examined in brainstem tissue obtained

from un-operated control, sham-operated, and SAH animals. As depicted in Fig. 1, a thick subarachnoid clot was typically observed along the ventral brainstem surface of SAH model animals. Following SAH, immunostaining of GFAP was markedly increased in tissue obtained 1–2 mm below the ventral surface of this brain region (Fig. 2a). The SAH-induced increase in GFAP immunostaining was paralleled by an increase in GFAP protein levels detected by Western blot (Fig. 2b). With both immunostaining and Western blot, GFAP detection was significantly elevated in tissue from 2-day and 5-day SAH animals compared to tissue obtained from un-operated and sham-operated animals. However, GFAP levels were not significantly different between 2-day and 5-day SAH animals. GFAP levels were similar between un-operated and sham-operated animals. These results demonstrate up-regulation of GFAP following SAH, consistent with the development of reactive astrogliosis.

Increased Astrocytic S100B Expression Following SAH

Upregulation and secretion of S100B, a Ca^{2+} binding protein selectively expressed in astrocytes, has been demonstrated in reactive astrocytes associated with several brain pathologies including traumatic brain injury and Alzheimer's disease [8]. We hypothesized that S100B is also elevated in the brain following SAH. The expected 196-bp RT–PCR product of S100B-specific primers was detected in brainstem from control and SAH animals (Fig. 3a). The expression of S100B mRNA relative to the house-keeping gene GAPDH was significantly greater in brainstem ($p<0.05$) from 5-day SAH animals compared to un-operated control and sham-operated animals ($n=5–6$ for each group). These data suggest elevated expression of S100B in brain parenchyma following SAH.

Enhanced Expression of HMGB1 in Brain Following SAH

S100B has recently been linked to microglial activation and inflammation within the brain [24]. We therefore examined whether SAH caused an up-regulation of the pro-inflammatory cytokine HMGB1 in microglia residing within brain parenchyma. HMGB1 is a non-histone DNA binding protein present in the nucleus under physiological conditions. However, during pathological events HMGB1 can be up-regulated, retained in the cytosol, and secreted by activated microglia as a pro-inflammatory cytokine [19,20]. As illustrated in Fig. 3b, HMGB1 mRNA was increased fivefold in brainstem from 5-day SAH compared to un-operated control or sham-operated animals ($p<0.05$). Further, a significant increase in HMGB1 protein was detected using Western blot in brainstem homogenates from 5-day SAH animals ($p<0.05$, Fig. 3c). These data demonstrate increased expression of HMGB1 in brain parenchyma following SAH.

Increased Cytosolic Expression of HMGB1 in Iba1-Positive Cells Following SAH

Immunohistochemistry studies were performed to determine whether cytosolic levels of HMGB1 were elevated in microglia of 5-day SAH animals. In brainstem sections from control animals, HMGB1 immunoreactivity overlapped with DAPI nuclear staining, consistent with the typical nuclear localization of HMGB1 (Fig. 4a, c). In marked contrast, cytosolic HMGB1 immunostaining was clearly evident in the cytosol of a sub-population of cells located within the brainstem of SAH animals (Fig. 4b, d). To gain insight into the identity of cells expressing cytosolic HMGB1, brainstem sections were co-immunostained using an antibody generated against Iba1, a specific marker for resident microglia and infiltrating macrophages [25]. The number of Iba1-positive cells was similar in brain from control and SAH animals, suggesting the majority of Iba1-positive cells represent resident microglial cells rather than infiltrating blood-derived macrophages (Fig. 4e–g). In brainstem from SAH model animals, approximately 90% of cells staining positively for Iba1 also stained positively for cytosolic HMGB1. These data demonstrate enhanced cytosolic

expression of pro-inflammatory HMGB1 in brain parenchyma of SAH model animals, occurring primarily in resident Iba1-positive cells.

Discussion

This study examined the impact of SAH on two types of glial cells within brain parenchyma, astrocytes, and microglia. Our data demonstrate that subarachnoid blood causes reactive astrogliosis, as evidenced by increased expression of two astrocyte-specific proteins, the intermediate filament GFAP, and the calcium binding protein S100B. Further, we provide novel evidence of SAH-induced up-regulation of the pro-inflammatory cytokine HMGB1 in the cytosol of resident microglia. Together, these findings demonstrate that SAH has a profound impact on glial cells within the brain.

The effect of reactive astrogliosis on brain function is enigmatic and controversial, with both protective and deleterious actions on neurons reported [7,26]. For example, reactive astrocytes have been reported to impart beneficial effects including decreased edema, preservation of the blood–brain barrier and protection of neurons from oxidative stress, enhanced glutamate release, and inflammatory damage. On the other hand, reactive astrocytes and the ensuing scar formation have also been reported to enhance the release of cytokines and limit axonal regeneration. The present study demonstrates that two hallmarks of reactive gliosis, enhanced expression of GFAP and S100B, are present in brain parenchyma obtained from SAH model animals. Surprisingly little is currently known regarding the development of reactive astrogliosis after aneurismal SAH [13], although elevated levels of S100B and GFAP have been reported in the serum and CSF of SAH patients [9–11]. Our current findings suggest reactive astrogliosis, rather than astrocyte cell death, underlies the elevated levels of GFAP and S100B detected in SAH patients. It remains to be resolved whether the severity of reactive gliosis and up-regulation of S100B and GFAP directly impact patient outcome, or simply reflect the severity of the initial brain insult (e.g., the volume of blood released onto the brain during aneurysm rupture). However, S100B has been implicated in microglial activation via binding to RAGE (receptors for advance glycation end products) [27] and stimulation of NFκB-dependent expression of pro-inflammatory molecules [28].

Consistent with SAH-induced microglial activation, we observed increased mRNA and protein levels of the pro-inflammatory cytokine HMGB1 in brainstem of SAH model animals. HMGB1 is a non-histone DNA binding protein normally present in the nucleus of neurons, astrocytes, microglia, and oligodendrocyte-like cells. However, under pathological conditions, activated microglia synthesize and actively secrete HMGB1, promoting brain inflammation [19,29]. For example, HMGB1 binding to RAGE has been shown to activate MAP kinase pathways and up-regulation of the transcription factor NFκB [27,30]. Previous studies have shown that HMGB1 translocates from the nucleus to the cytoplasm and is released extracellularly from activated microglia [29] as well as from blood-derived monocytes that can further differentiate into macrophages within the brain [31]. Consistent with these reports, our data demonstrate a dramatic increase in cytosolic HMGB1 expression after SAH. Cells from SAH animals expressing cytoplasmic HMGB1 also immunostained positively with an antibody against Iba1, a protein selectively expressed in microglia and macrophages [25]. Iba1 immunostaining cannot distinguish between resident microglia and infiltrating macrophages. However, we observed a similar density of Iba1-positive cells in control and SAH brain, suggesting up-regulation of cytosolic HMGB1 primarily occurred in activated microglia rather than monocytes infiltrating from either the clot or bloodstream.

Evidence is rapidly accumulating to suggest that HMGB1 may play an important role in brain injury following stroke. Muhammad et al. [32] have demonstrated, using a mouse

middle cerebral artery occlusion model, that HMGB1 engagement of RAGE triggers inflammation and infarction leading to ischemic brain injury. Recent studies have also reported elevated HMGB1 levels in the CSF of SAH patients with poor outcome [17,18]. To our knowledge, our present studies represent the first report of elevated cytosolic HMGB1 in brain parenchyma of SAH animals. Our results suggest SAH elevates extracelluar HMGB1 levels via a pathway involving microglial activation and secretion of cytosolic HMGB1. Further, as HMGB1 and S100B are both ligands for RAGE and co-regulate apoptosis [27], we propose that these proteins may act in concert to promote brain inflammation following SAH.

Conclusion/Summary

In summary, the present study demonstrates profound effects of SAH on glial cells leading to reactive astrogliosis and microglial activation. Up-regulation of pro-inflammatory molecules S100B and HMGB1 may contribute to pathological changes in the brain following cerebral aneurysm rupture and subarachnoid hemorrhage.

Acknowledgments

The authors would like to thank Bryce Bludevich, Kevin P. O'Connor, Matthew A. Nystoriak, Edward Zelazny, Todd Clason, Richard A. Hughes, and Keith K. Locke for their helpful comments and assistance with this study. This work was supported by the Totman Medical Research Trust Fund, the Peter Martin Brain Aneurysm Endowment, and NIH NHLBI (R01 HL078983 and P01 HL095488). Research on this project was conducted with the aid of the COBRE Imaging and Cell/Molecular core facilities, which are supported by Grant Number P20 RR016435 from the National Center for Research Resources (NCRR), a component of the National Institutes of Health (NIH).

References

1. Hop JW, Rinkel GJ, Algra A, van Gijn J. Case-fatality rates and functional outcome after subarachnoid hemorrhage: a systematic review. Stroke. 1997; 28:660–4. [PubMed: 9056628]
2. Hansen-Schwartz J, Vajkoczy P, Macdonald RL, Pluta RM, Zhang JH. Cerebral vasospasm: looking beyond vasoconstriction. Trends Pharmacol Sci. 2007; 28:252–6. [PubMed: 17466386]
3. Pluta RM, Hansen-Schwartz J, Dreier J, Vajkoczy P, Macdonald RL, Nishizawa S, et al. Cerebral vasospasm following subarach-noide hemorrhage: time for a new world of thought. Neurol Res. 2009; 31:151–8. [PubMed: 19298755]
4. Sabri M, Kawashima A, Ai J, Macdonald RL. Neuronal and astrocytic apoptosis after subarachnoid hemorrhage: a possible cause for poor prognosis. Brain Res. 2008; 1238:163–71. [PubMed: 18786513]
5. Vergouwen MD, Vermeulen M, Coert BA, Stroes ES, Roos YB. Microthrombosis after aneurysmal subarachnoid hemorrhage: an additional explanation for delayed cerebral ischemia. J Cereb Blood Flow Metab. 2008; 28:1761–70. [PubMed: 18628782]
6. Wellman GC. Ion channels and calcium signaling in cerebral arteries following subarachnoid hemorrhage. Neurol Res. 2006; 28:690–702. [PubMed: 17164032]
7. Pekny M, Nilsson M. Astrocyte activation and reactive gliosis. Glia. 2005; 50:427–34. [PubMed: 15846805]
8. Sen J, Belli A. S100B in neuropathologic states: the CRP of the brain? J Neurosci Res. 2007; 85:1373–80. [PubMed: 17348038]
9. Nylen K, Csajbok LZ, Ost M, Rashid A, Blennow K, Nellgard B, et al. Serum glial fibrillary acidic protein is related to focal brain injury and outcome after aneurysmal subarachnoid hemorrhage. Stroke. 2007; 38:1489–94. [PubMed: 17395862]
10. Petzold A, Keir G, Lim D, Smith M, Thompson EJ. Cerebrospinal fluid (CSF) and serum S100B: release and wash-out pattern. Brain Res Bull. 2003; 61:281–5. [PubMed: 12909298]

11. Petzold A, Keir G, Kerr M, Kay A, Kitchen N, Smith M, et al. Early identification of secondary brain damage in subarachnoid hemorrhage: a role for glial fibrillary acidic protein. J Neurotrauma. 2006; 23:1179–84. [PubMed: 16866629]
12. Pereira AR, Sanchez-Pena P, Biondi A, Sourour N, Boch AL, Colonne C, et al. Predictors of 1-year outcome after coiling for poor-grade subarachnoid aneurysmal hemorrhage. Neurocrit Care. 2007; 7:18–26. [PubMed: 17657653]
13. Yokota M, Peterson JW, Tani E, Yamaura I. The immunohisto-chemical distribution of protein kinase C isozymes is altered in the canine brain and basilar artery after subarachnoid hemorrhage. Neurosci Lett. 1994; 180:171–4. [PubMed: 7700574]
14. Dumont AS, Dumont RJ, Chow MM, Lin CL, Calisaneller T, Ley KF, et al. Cerebral vasospasm after subarachnoid hemorrhage: putative role of inflammation. Neurosurgery. 2003; 53:123–33. [PubMed: 12823881]
15. Prunell GF, Svendgaard NA, Alkass K, Mathiesen T. Inflammation in the brain after experimental subarachnoid hemorrhage. Neurosurgery. 2005; 56:1082–92. [PubMed: 15854258]
16. Simard JM, Geng Z, Woo SK, Ivanova S, Tosun C, Melnichenko L, et al. Glibenclamide reduces inflammation, vasogenic edema, and caspase-3 activation after subarachnoid hemorrhage. J Cereb Blood Flow Metab. 2009; 29:317–30. [PubMed: 18854840]
17. King MD, Laird MD, Ramesh SS, Youssef P, Shakir B, Vender JR, et al. Elucidating novel mechanisms of brain injury following subarachnoid hemorrhage: an emerging role for neuroproteomics. Neurosurg Focus. 2010; 28:E10. [PubMed: 20043714]
18. Nakahara T, Tsuruta R, Kaneko T, Yamashita S, Fujita M, Kasaoka S, et al. High-mobility group box 1 protein in CSF of patients with subarachnoid hemorrhage. Neurocrit Care. 2009; 11:362–8. [PubMed: 19777384]
19. Hayakawa K, Mishima K, Nozako M, Hazekawa M, Mishima S, Fujioka M, et al. Delayed treatment with minocycline ameliorates neurologic impairment through activated microglia expressing a high-mobility group box1-inhibiting mechanism. Stroke. 2008; 39:951–8. [PubMed: 18258837]
20. Kim JB, Sig CJ, Yu YM, Nam K, Piao CS, Kim SW, et al. HMGB1, a novel cytokine-like mediator linking acute neuronal death and delayed neuroinflammation in the postischemic brain. J Neurosci. 2006; 26:6413–21. [PubMed: 16775128]
21. Ishiguro M, Puryear CB, Bisson E, Saundry CM, Nathan DJ, Russell SR, et al. Enhanced myogenic tone in cerebral arteries from a rabbit model of subarachnoid hemorrhage. Am J Physiol Heart Circ Physiol. 2002; 283:H2217–25. [PubMed: 12388249]
22. Ishiguro M, Wellman TL, Honda A, Russell SR, Tranmer BI, Wellman GC. Emergence of a R-type Ca^{2+} channel (Ca_V 2.3) contributes to cerebral artery constriction after subarachnoid hemorrhage. Circ Res. 2005; 96:419–26. [PubMed: 15692089]
23. Eng LF, Ghirnikar RS, Lee YL. Glial fibrillary acidic protein: GFAP—thirty-one years (1969–2000). Neurochem Res. 2000; 25:1439–51. [PubMed: 11059815]
24. Bianchi R, Adami C, Giambanco I, Donato R. S100B binding to RAGE in microglia stimulates COX-2 expression. J Leukoc Biol. 2007; 81:108–18. [PubMed: 17023559]
25. Ito D, Tanaka K, Suzuki S, Dembo T, Fukuuchi Y. Enhanced expression of Iba1, ionized calcium-binding adapter molecule 1, after transient focal cerebral ischemia in rat brain. Stroke. 2001; 32:1208–15. [PubMed: 11340235]
26. Sofroniew MV. Reactive astrocytes in neural repair and protection. Neuroscientist. 2005; 11:400–7. [PubMed: 16151042]
27. Huttunen HJ, Kuja-Panula J, Sorci G, Agneletti AL, Donato R, Rauvala H. Coregulation of neurite outgrowth and cell survival by amphoterin and S100 proteins through receptor for advanced glycation end products (RAGE) activation. J Biol Chem. 2000; 275:40096–105. [PubMed: 11007787]
28. Donato R. S100: a multigenic family of calcium-modulated proteins of the EF-hand type with intracellular and extracellular functional roles. Int J Biochem Cell Biol. 2001; 33:637–68. [PubMed: 11390274]

29. Kim JB, Lim CM, Yu YM, Lee JK. Induction and subcellular localization of high-mobility group box-1 (HMGB1) in the postischemic rat brain. J Neurosci Res. 2008; 86:1125–31. [PubMed: 17975839]

30. Taguchi A, Blood DC, del Toro G, Canet A, Lee DC, Qu W, et al. Blockade of RAGE-amphoterin signalling suppresses tumour growth and metastases. Nature. 2000; 405:354–60. [PubMed: 10830965]

31. Gardella S, Andrei C, Ferrera D, Lotti LV, Torrisi MR, Bianchi ME, et al. The nuclear protein HMGB1 is secreted by monocytes via a non-classical, vesicle-mediated secretory pathway. EMBO Rep. 2002; 3:995–1001. [PubMed: 12231511]

32. Muhammad S, Barakat W, Stoyanov S, Murikinati S, Yang H, Tracey KJ, et al. The HMGB1 receptor RAGE mediates ischemic brain damage. J Neurosci. 2008; 28:12023–31. [PubMed: 19005067]

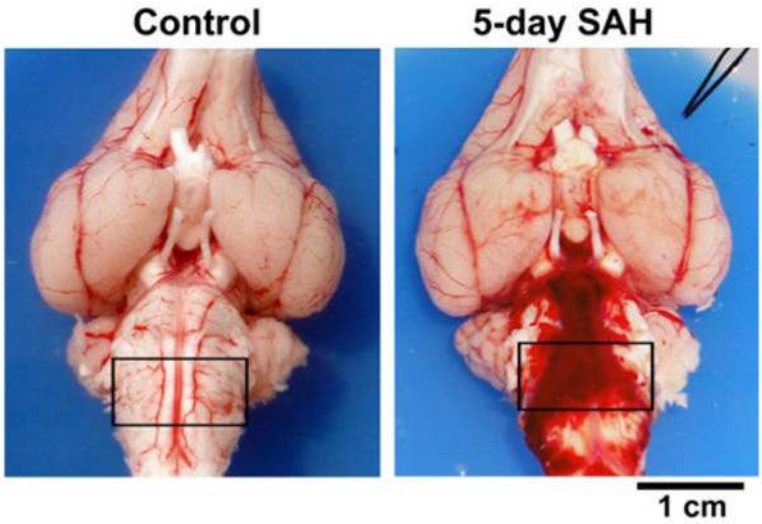

Fig. 1.

Distribution of blood following experimental SAH in rabbits. Ventral view of brains obtained from a healthy control (*left panel*) and a 5-day SAH animal (*right panel*). Brainstem tissue, used throughout this study, was obtained 1–2 mm below the brain surface from regions denoted by *black rectangular boxes*

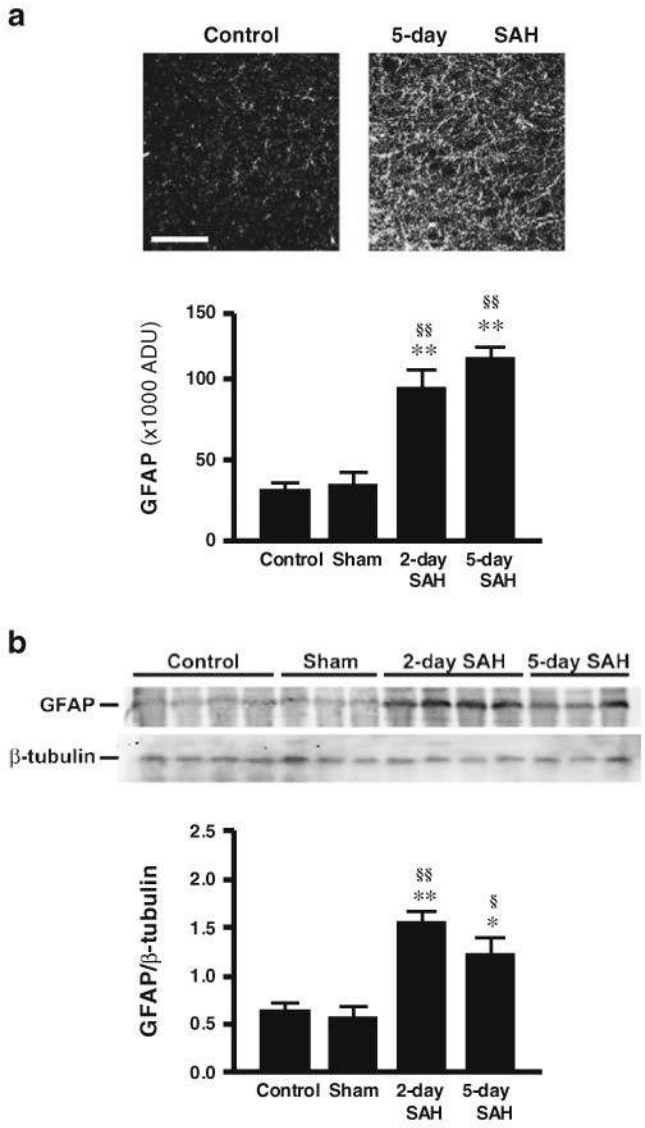

Fig. 2.

Enhanced expression of glial fibrillary acidic protein (*GFAP*) in brainstem from SAH model animals. **a** GFAP immunostaining is increased in brainstem from SAH model animals. Images demonstrate enhanced GFAP immunostaining in brainstem obtained from a 5-day SAH animal. *Bar graph* expresses GFAP immunostaining, in arbitrary density units (ADU), in tissue obtained from un-operated control (n= 6), 5-day sham-operated (n=4), 2-day SAH (n=4), and 5-day SAH (n=6) animals. Three images per animal were randomly selected for analysis. *Scale bar*: 50 μm. $^{**}p<0.01$ versus control and $\S\S p<0.01$ versus sham using Tukey–Kramer multiple comparison test. **b** GFAP protein is increased in brainstem following SAH. Western blot demonstrating immunoreactive bands corresponding to GFAP and β-tubulin using 5 μg of protein obtained from control (n=4), sham-operated (n=3), 2-day SAH (n=4), and 5-day SAH (n=3) brainstem. GFAP band intensity was quantified using NIH software (ImageJ) and expressed as a ratio to β-tubulin band intensity. $^{**}p<0.01$, $^{*}p<0.05$, versus control and $\S\S p<0.01$, $\S p<0.05$ versus sham using Tukey–Kramer multiple comparison test

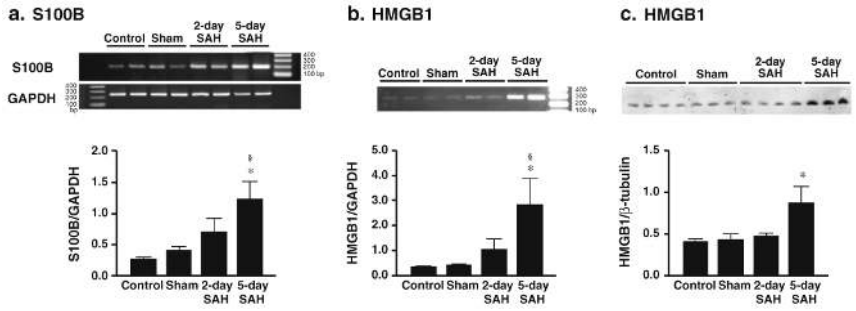

Fig. 3.

Enhanced expression of S100B and HMGB1 in brainstem from SAH rabbits. **a** *Top panel* representative image of an RT–PCR gel using S100B- and GAPDH-specific primers. *Bottom panel* summarized RT–PCR data obtained from RNA isolated from brainstem of control (*n*=5), sham-operated (*n*=5), 2-day SAH (*n*=6), and 5-day SAH (*n*=6) animals using quantitative densitometric analysis. S100B band intensity is expressed relative to GAPDH band intensity for each animal. **b** *Top panel* representative image of an RT–PCR gel using HMGB1-specific primers. *Bottom panel* quantification of HMGB1 mRNA in brainstem from control (*n*=5), sham-operated (*n*=5), 2-day (*n*=4), and 5-day SAH (*n*=5) animals. Data were obtained using quantitative densitometric analysis of RT–PCR gels. HMGB1 band intensity is expressed relative to GAPDH band intensity for each animal. **c** *Top panel* Western blot demonstrating immunoreactive bands corresponding to HMGB1 using 5 μg of protein obtained from control, sham-operated, 2-day SAH, and 5-day SAH brainstem. *Bottom panel* quantification of HMGB1 protein levels in brainstem from control (*n*=4), sham-operated (*n*=3), 2-day (*n*=4), and 5-day SAH (*n*=3) animals obtained using Western blot. HMGB1 band intensity was quantified using NIH software (ImageJ) and expressed as a ratio to β-tubulin band intensity. **p*<0.05 versus control and §*p*<0.05 versus sham using Tukey–Kramer multiple comparison test

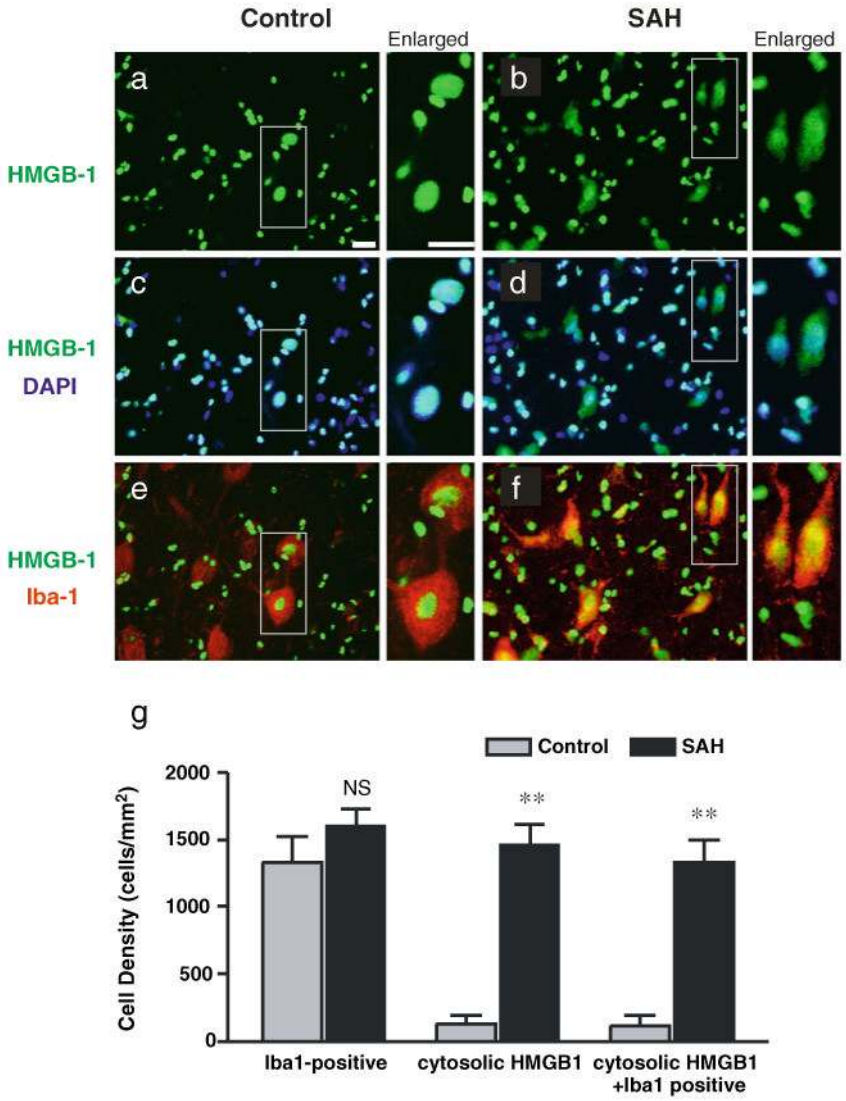

Fig. 4.

Cytosolic expression of HMGB1 in Iba1-positive cells of brainstem from SAH animals. **a, b** HMGB1 immunostaining images obtained from brainstem of a control (**a**) and a 5-day SAH (**b**) animal. **c, d** Merged images of HMGB1 immunos-taining (*green*) and DAPI nuclear staining (*blue*). **e, f** Merged images of HMGB1 immunostaining (*green*) and Iba1 immunostaining (*red*). Enlarged images on the *right side* of each panel highlight the increased number of Iba1-positive cells with cytosolic staining of HMGB1 in brainstem from SAH animals. *Scale bars* represent 5 μm. **g** Quantification of the density of cells staining positively for Iba1 and cytosolic HMGB1. Values were obtained from averaging three to four brainstem images per animal (n=4 animals per group). $^{**}p<0.01$, Student t test